Disruption runaway electron generation and mitigation in the Spherical Tokamak for Energy Production (STEP)

(article starts on next page)

PAPER • OPEN ACCESS

Disruption runaway electron generation and mitigation in the Spherical Tokamak for Energy Production (STEP)

To cite this article: A. Fil *et al* 2024 *Nucl. Fusion* **64** 106049

View the article online for updates and enhancements.

Disruption runaway electron generation and mitigation in the Spherical Tokamak for Energy Production (STEP)

A. Fil[1,2,*] , L. Henden[1], S. Newton[1], M. Hoppe[3] and O. Vallhagen[4]

[1] United Kingdom Atomic Energy Authority, Culham Campus, Abingdon, Oxon OX14 3DB, United Kingdom of Great Britain and Northern Ireland
[2] CEA, IRFM, F-13108 Saint-Paul-lez-Durance, France
[3] Department of Electrical Engineering, KTH Royal Institute of Technology, Stockholm, Sweden
[4] Department of Physics, Chalmers University of Technology, SE-41296 Gothenburg, Sweden

E-mail: alexandre.fil@cea.fr and alexandre.fil@ukaea.uk

CrossMark

Abstract

Generation of Runaway Electrons (REs) during plasma disruptions is of great concern for ITER and future reactors based on the tokamak concept. Unmitigated RE generation in the current STEP (Spherical Tokamak for Energy Production) concept design is modelled using the code DREAM, with hot-tail generation found to be the dominant primary generation mechanism and avalanche multiplication of REs found to be extremely high. Varying assumptions for the prescribed thermal quench (TQ) phase (duration, final electron temperature) as well as the wall time, the plasma-wall distance, and shaping effects, all STEP full-power and full-current unmitigated disruptions generate large RE beams (from 10 MA up to full conversion). RE mitigation is first studied by modelling idealised mixed impurity injections, with ad-hoc particle transport arising from the stochasticity of the magnetic field during the TQ, but no combination of argon and deuterium quantities allows runaways to be avoided while respecting the other constraints of disruption mitigation. Initial concept of STEP disruption mitigation system is then tested with DREAM, assuming two-stage shattered pellet injections (SPI) of pure D_2 followed by $Ar+D_2$. Such a scheme is found to reduce the generation of REs by the hot-tail mechanism, but still generates a RE beam of about 13 MA. Options for further optimising the SPI scheme, for mitigating a large RE beam in STEP (benign termination scheme), as well as estimations of required RE losses during the current quench (from a potential passive RE mitigation coil) will also be discussed.

(Some figures may appear in colour only in the online journal)

---

* Author to whom any correspondence should be addressed.

1. Introduction

Generation of Runaway Electrons (REs) during plasma disruptions, and their potential impact on the plasma facing components (PFCs), is of great concern for ITER [1] and future reactors based on the tokamak concept. The STEP (Spherical Tokamak for Energy Production) programme [2] aims at producing net energy from a prototype fusion energy plant. Its current flat top operating point features a plasma current higher than 20 MA, and is thus expected to be in a regime with very high avalanche multiplication, i.e. even small runaway seeds would quickly generate a large runaway beam during unmitigated current quenches. Indeed, recent studies of ITER [3], SPARC [4] and of a smaller STEP concept [5] have shown that such plasmas are prone to large RE beams during disruptions, even when mitigated (by deuterium, argon or neon single or multiple injections). Several modelling tools have been developed in the past few years to better model the generation of REs, including NIMROD [6], M3D-C1 [7], JOREK [8], MARS-F [9], and the code used in this study: DREAM [10]. Most of those codes are 3D non-linear MHD codes, computationally expensive, and more suitable for the modelling of existing experiments or an already well-defined scenario. As STEP is still in the concept design phase, a faster, modular, open-source code such as DREAM is a powerful tool to quickly explore and map the operational space of STEP Disruption Mitigation System (DMS). DREAM is modular in the sense that it can be run with different models for runaways and the background plasma population, i.e. as in fluid, isotropic or fully kinetic. More details on the models and their assumptions can be found in [5] or [10]. DREAM can use prescribed temperature profiles, a feature which will be used to model unmitigated disruptions in section 2, or have a self-consistent temperature evolution (including impurities). The latter will be used to explore runaway generation in STEP for varying injected impurity densities in section 3. DREAM also includes a model for Shattered Pellet Injection (or SPI) [3], that will be used extensively in section 4 to test the initial STEP DMS concept design. In this paper, we use DREAM in fully fluid mode (as in [5]), the implication of this assumption (and other assumptions of the modelling) will be discussed in section 5, as well as some discussion on how STEP plans to mitigate predicted high-current RE beams.

2. RE generation in STEP unmitigated disruptions

All simulations presented in this paper start from a STEP flat top operating point (so called 'STEP-EC-HD-v3') obtained using the integrated modelling tool JETTO [2]. This workflow provides DREAM with initial profiles for the plasma density, temperature and parallel current density. Main parameters are: major radius $R_0 = 3.6$ m, minor radius $a = 2$ m, toroidal magnetic field at the magnetic axis $B_{T,0} = 3.2$ T, total plasma current $I_p \simeq 20$ MA, core electron temperature $T_{e,0} \simeq 18$ keV, core electron density $n_{e,0} \simeq 1.5 \cdot 10^{20}$ m^{-3}, resulting in total
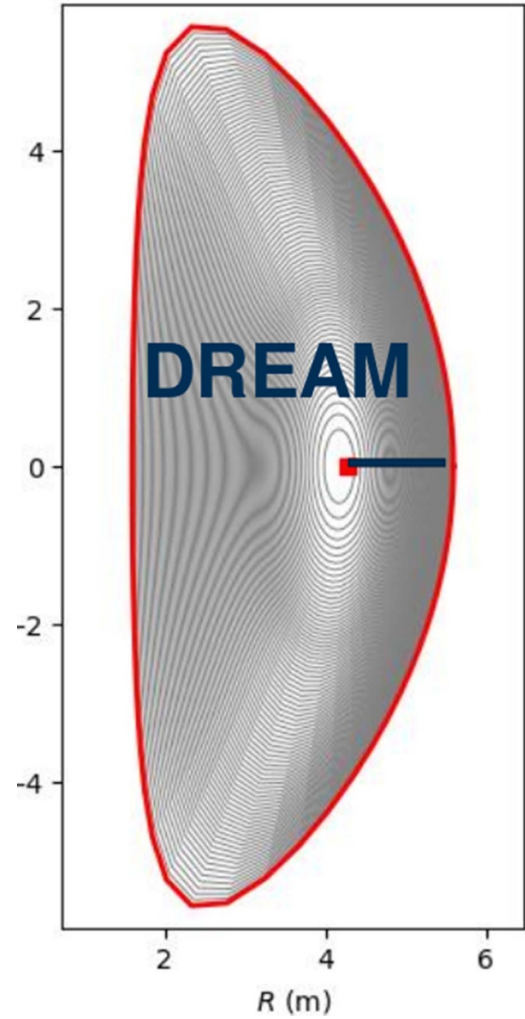

Figure 1. STEP-EC-HD-v3 equilibrium and sketch of DREAM 1D radial domain (flux surface averaged).

thermal and magnetic energies of $E_{th} = 580$ MJ and $E_{mag} = 127$ MJ. A free-boundary equilibrium file is provided by the code FIESTA [11], from which Miller parameters [12] (i.e. triangularity, elongation $\kappa \simeq 3$, Shafranov shift, etc) are extracted, either using DREAM tools or the python library pyrokinetics. STEP flux surfaces (kept intact throughout the simulations), Miller parameters and initial plasma profiles are shown in figures 1 and 2, as well as the DREAM simulation domain. DREAM is a flux-surface averaged code, thus simulating only across the radial coordinate, but is able to include the effect of shaping. The elongation in particular has been found to reduce the generation of REs in previous studies [13] and the shaping is included in the simulations of sections 2 and 3. A conformal wall is also included, with a plasma-wall gap of $d_{wall} = 20$ cm and a wall time of $\tau_{wall} = 50$ ms for most of the simulations presented in this paper. Regarding RE generation mechanisms, state-of-the-art fluid rates are used for Dreicer [14], hot-tail [10] and avalanche [15]. Tritium β decay and Compton scattering are not included in most simulations presented in
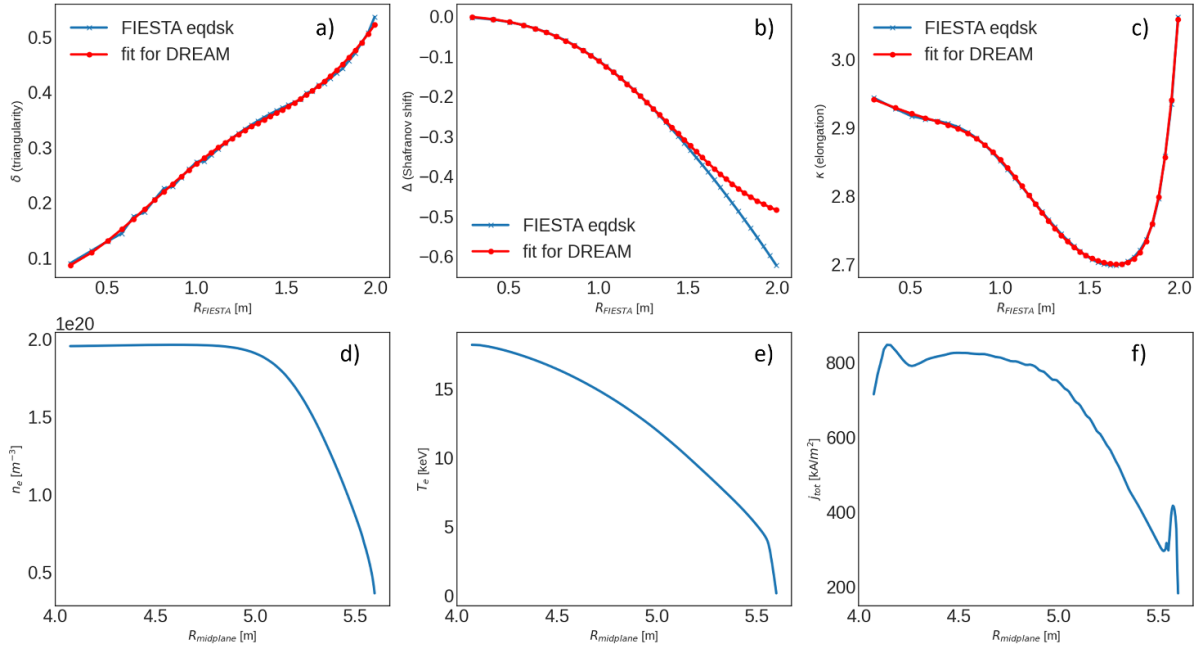
Figure 2. Top: STEP-EC-HD-v3 Miller parameters ((*a*) triangularity, (*b*) Shafranov shift, (*c*) elongation) extracted from FIESTA free-boundary equilibrium (blue), and values used in DREAM (red). Note the modification of the Shafranov shift, to avoid a magnetic well on the LFS (which cannot be modelled by DREAM). Bottom: JETTO STEP-EC-HD-v3 electron density (*d*) and temperature (*e*), as well as total current density (*f*), used as initial conditions for the DREAM simulations.

this paper, but usually increase the primary RE generation in STEP active phase (as will be discussed in section 5). While the temperature evolution will be self-consistent in the following sections, we start by modelling unmitigated disruptions with a prescribed temperature evolution, i.e. by specifying a thermal quench (TQ) time (t_{TQ}) and a final electron temperature ($T_{e,final}$).

Figure 3 shows the evolution of the total plasma current I_p, the Ohmic current I_{Ohm} and the RE current I_{RE} for a prescribed TQ with $t_{TQ} = 3.4$ ms and $T_{e,final} = 10$ eV. The prescribed TQ is followed by a current quench lasting $t_{CQ} \simeq 117$ ms, during which a RE plateau with a RE current of 14.7 MA is formed. The conversion rate between the initial plasma current and the final RE current ($CR = I_{RE,final}/I_{p,0}$) is found to be 74% in that particular case. Because of the uncertainties on STEP TQ characteristics, scans of the prescribed parameters have been performed, i.e. t_{TQ}[ms] $\in [0.6-10]$, $T_{e,final}$[eV] $\in [1-60]$, d_{wall}[m] $\in [0.1-0.5]$, τ_{wall}[ms] $\in [10-500]$. Depending on those the final RE current can vary significantly, between 10 MA and full conversion ($I_{RE} \simeq 20$ MA), with the shorter and colder TQ inducing the highest RE beam currents. Hot-tail is generally the dominant primary generation mechanism and the avalanche generation rate is orders of magnitude higher than all the other generation rates, as can be seen in figure 4 for the simulation with $t_{TQ} = 3.4$ ms and $T_{e,final} = 10$ eV. While shaping effects (i.e. elongation, etc) are included in those simulations, the same scans in TQ parameters have also been done in cylindrical geometry. Those generally have a higher maximum electric field and a final RE current 10%–20% higher, which is consistent with [5, 13] (for conventional tokamaks).

3. Idealised impurity injections

Disruption mitigation by idealised, i.e. radially uniform, impurity injection of a mixture of argon and deuterium is now modelled, with RE transport arising from the disruption of the magnetic flux surfaces (i.e. Rechester–Rosenbluth [16]). Note that injections of a mixture of neon and deuterium have also been performed, showing a lower generation of runaways compared to the simulations shown below (likely due to the lower number of bound electrons acting as a runaway source during avalanche). However, recent indications of argon being easier to purge for benign RE beam termination [17] and fuel cycle considerations (argon is already used for divertor seeding to achieve plasma detachment) promote the use of argon in STEP. We will thus only discuss argon (and deuterium) injections in the rest of the paper.

Unlike section 2, the energy balance equation given in [10] is now solved, using radiation/ionisation/recombination coefficients from AMJUEL (Atomic and Molecular data that was computed for the EIRENE code, see www.eirene.de/ Documentation/amjuel.pdf) accounting for opacity to Lyman radiation. Impurities are initially deposited uniformly in the plasma (as in [5]). This impurity injection is clearly idealised, but is useful to find what core densities would be needed to prevent hot-tail generation of REs and reduce as much as possible the final RE current. Figure 5 shows an example of such a simulation: after a first phase lasting 1 μs to initialise the profiles (see figures 2(*a*) and (*e*)) for initial n_e and T_e profiles) and get a self-consistent electric field, the impurities are added. In the simulation shown on figure 5, $n_{Ar} = 5 \cdot 10^{18}$ m^{-3},
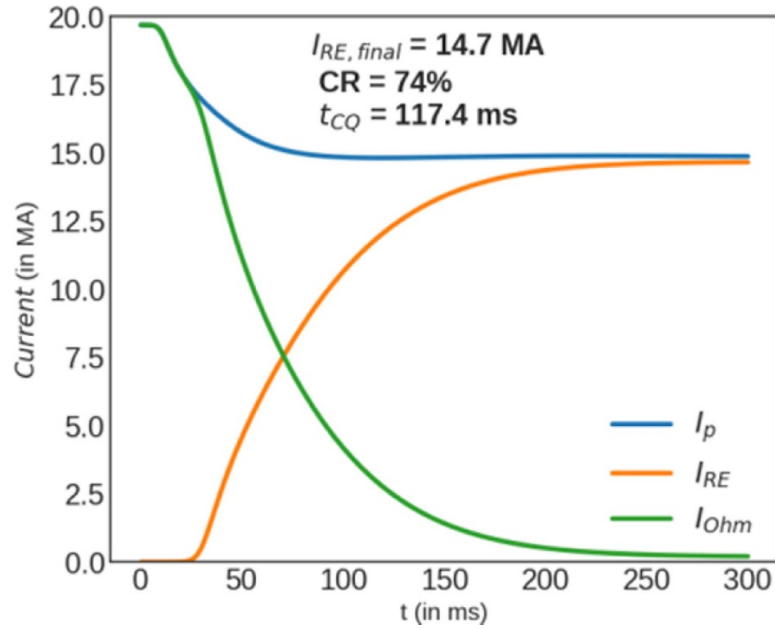
Figure 3. Evolution of the total plasma current, ohmic and runaway electron current in STEP-EC-HD-v3 unmitigated disruption with prescribed TQ ($t_{TQ} = 3.4$ ms and $T_{e,final} = 10$ eV). A runaway electron beam of 14.7 MA is observed.
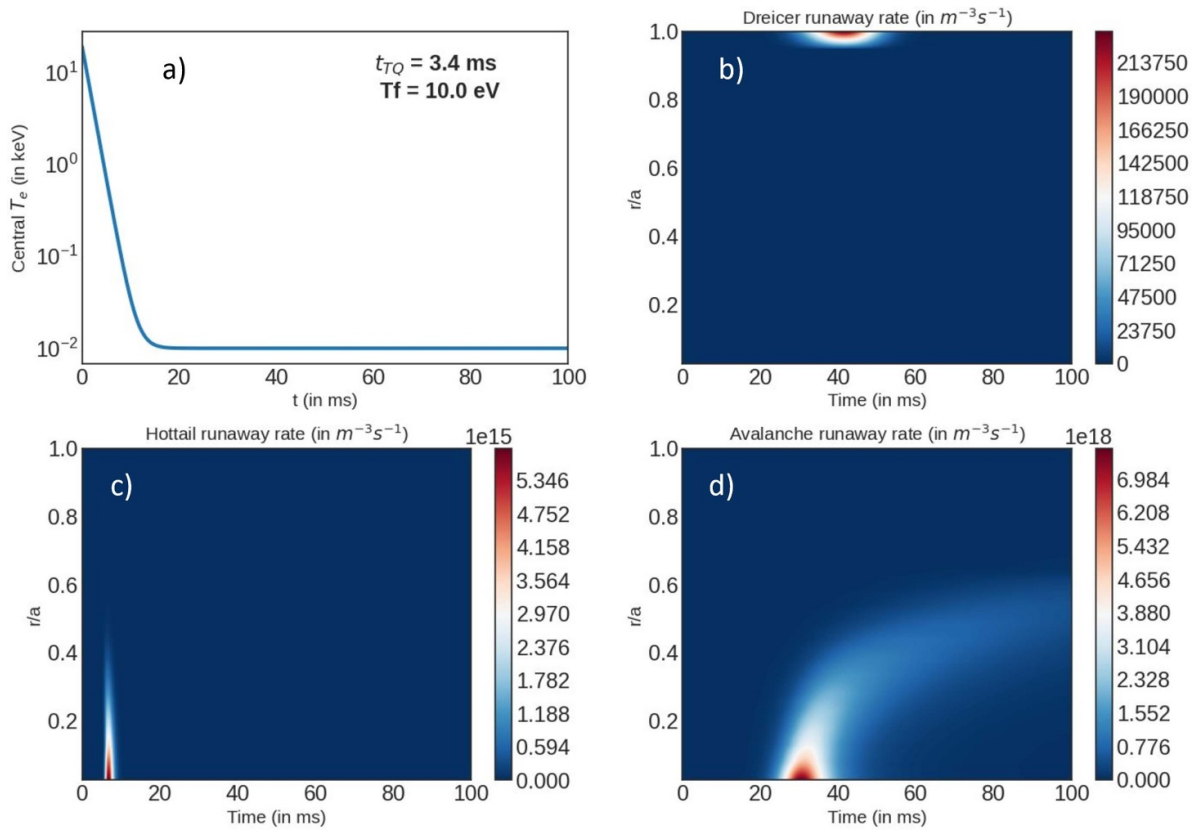
Figure 4. Core electron temperature (*a*) and runaway electron generation rates (from (*b*) Dreicer, (*c*) Hot-tail and (*d*) Avalanche) for a STEP unmitigated disruption with prescribed TQ of $t_{TQ} = 3.4$ ms and $T_{e,final} = 10$ eV, i.e. same simulation as in figure 3.

$n_{D_2} = 10^{21}$ m^{-3} is used. The plasma is diluted by the large quantities of deuterium injected (see central temperature in red on figure 5(*a*), and then argon radiates most of the thermal energy (see figures 5(*a*) and (*d*)). We also use an ad-hoc TQ

thermal transport coefficient, to represent that caused by magnetic stochasticity during the TQ, with normalised perturbation $\delta B/B = 2 \cdot 10^{-3}$ (such a level is consistent with ITER 3D non-linear MHD modelling [18]). This reduces the plasma

Figure 5. Idealised impurity injection case using an $Ar + D_2$ mixture ($n_{Ar} = 5 \cdot 10^{18}\,m^{-3}$, $n_{D_2} = 10^{21}\,m^{-3}$). Rechester–Rosenbluth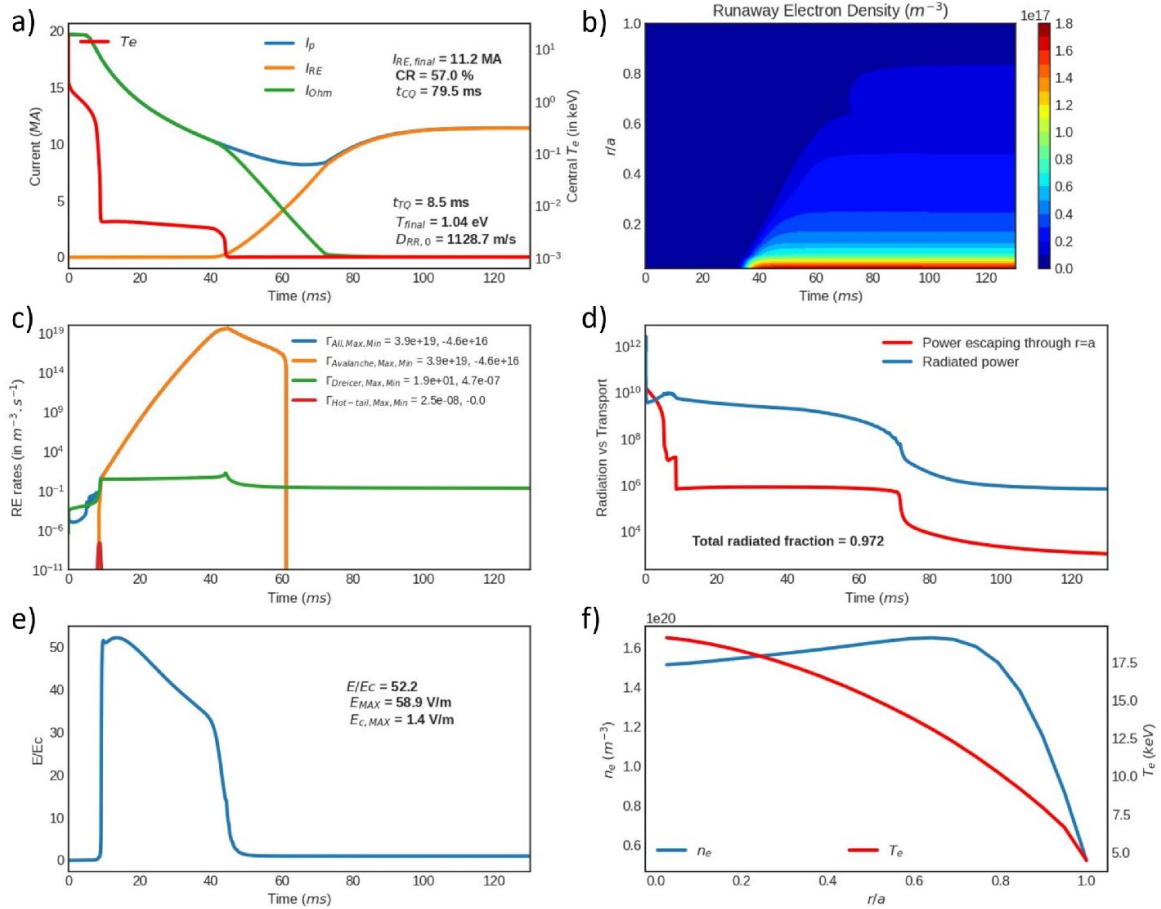 transport with a magnetic perturbation of $\delta B/B = 2 \cdot 10^{-3}$ is active during ionisation and thermal quench phases. (*a*) Central electron temperature evolution and total, ohmic and runaway currents. (*b*) Evolution of the RE density profile. (*c*) Evolution of the integrated RE generation rates. (*d*) Evolution of the power escaping through the outer boundary and the integrated radiated power. (*e*) Evolution of the parallel electric field divided by the effective critical electric field for RE generation. (*f*) Initial electron density and temperature profiles.

electron temperature to about 1 eV. Note that during the TQ, both Dreicer and hot-tail generation are more than 10 orders of magnitude smaller than in the unmitigated cases of section 2 (see figure 5(*c*)) and the injection thus fulfills its main purpose. The current quench then occurs (see figure 5(*a*)), with the parallel electric field increasing up to 60 V m^{-1} (as can be seen in figure 5(*e*), which shows the ratio of the parallel electric field with the effective critical electric field for RE generation, as derived in [19]). During the phase with high electric field, the RE population starts quite small but progressively grows through avalanche, before forming a large population of REs 30–40 ms after the beginning of the CQ (see the RE density on figure 5(*b*) and a large 11.2 MA RE beam (see figure 5(*a*)).

Scanning the injected argon neutral density ($n_{Ar}[m^{-3}] \in [5 \cdot 10^{17} - 10^{20}]$) and deuterium neutral density ($n_{D_2}[m^{-3}] \in [10^{20} - 10^{22}]$), we obtain a final RE current between 15 MA and 8 MA, as shown in figure 6(*a*). This is much higher than the LOCA (Loss of Coolant Accident) $I_{RE} = 0.5$ MA limit in the most recent ITER DMS specification [20]. While a similar limit is not yet well defined for STEP, such a RE beam will likely cause significant damage to PFCs and must be

mitigated by additional systems (for example through pure deuterium SPI into the RE beam to get a benign termination [21]). Additionally, the smallest RE beams are achieved for relatively low densities of argon, which are not compatible with the DMS constraints on radiation fraction and on CQ time (i.e. radiation fraction above 90% to avoid localised melting of PFCs, and current quench time between 20 and 120 ms to avoid the largest electromagnetic forces in conducting structures; see figures 6(*b*) and (*d*)). Too much argon and deuterium also decreases the CQ time too much (and thus increases induced eddy currents and resulting forces in conducting structures) and shortens the radiation flash during disruption mitigation, increasing the peak Heat Impact Factor (HIF) above the tungsten melt limit of 60 MJ·m^{-2}·s$^{-0.5}$ [22] (see figure 6(*c*)). Figure 6(*e*) plots a normalised overlap parameter taking those constraints into account, to find an optimal injection density of $n_{Ar} \simeq 10^{18}\,m^{-3}$, $n_{D_2} \simeq 10^{21}\,m^{-3}$ (green star) which fulfills all non-RE DMS constraints (but with a RE beam current above 10 MA). Unlike previous simulations of RE mitigation in a ST, published in [5], no RE-free domain has been found. This is due to a combination of effects, in particular a lower amplitude and shorter TQ
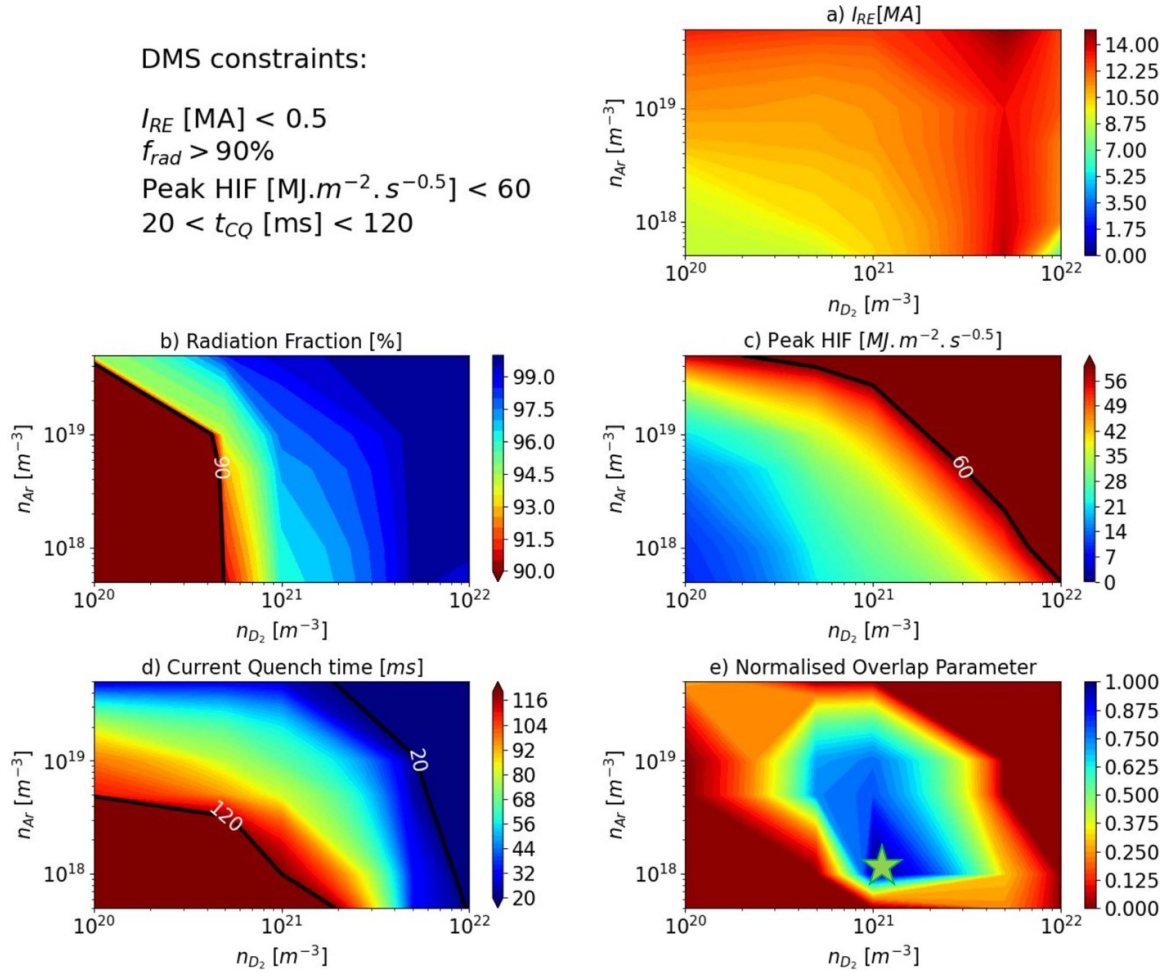
Figure 6. Idealised impurity injection scan using an Ar+D$_2$ mixture. Rechester–Rosenbluth transport with a magnetic perturbation of $\delta B/B = 2 \cdot 10^{-3}$ is active during ionisation and thermal quench phases. (*a*) shows that the runaway current after 200 ms is above the limit in all cases; (*b*) the total radiation fraction; (*c*) the peak heat impact factor on the first wall during the radiation flash; (*d*) the current quench time; For (*b*)–(*d*), everything which is out of the colourbar range (i.e. outside of the black lines indicating the limits, for example minimum 90% radiation fraction in (*b*)) does not fulfill the DMS constraint. The limit is not visible in (*a*), as I_{RE} is always above 0.5 MA. (*e*) shows the normalised overlap parameter which combines the DMS constraints (blue is good, red is bad, and the RE constraint is not fulfilled in any case).

$\delta B/B$ in our paper (thus lower sink term for REs), the use of argon instead of neon, and a more realistic plasma-wall distance.

4. Testing STEP DMS concept design using DREAM SPI model

More realistic particle deposition profiles can substantially impact the results [3], and STEP initial DMS concept design needs to be tested in terms of pellet assimilation into the plasma. In particular, recent studies for ITER with the code INDEX [23] have shown that large pellets (such as planned for STEP) may not be fully assimilated by the target plasma, which would greatly constrain the parameter space explored in the previous section. DREAM SPI model has been benchmarked against INDEX (without plasmoid drifts) and JOREK,

and is thus also used in this section. We model a two-stage SPI scheme, as in ITER [3], with dilution cooling from pure D$_2$ pellets followed by a strongly radiating phase due to mixed Ar + D$_2$ pellets. Note that in STEP, the pure D$_2$ injectors are planned on the High-Field-Side of the device, to make use of plasmoid drifts and improve assimilation of those pellets (compared to what will be modelled in the following, where pellet drifts are not taken into account). We scan the injection parameters of the initial STEP DMS concept design, which consists of 12 injectors of 22 mm pure D$_2$ pellets for RE Avoidance (stage 1), 15 injectors of mixed Ar+D$_2$ 16 mm pellets for TQ/CQ mitigation (stage 2), and 30 injectors of pure D$_2$ 7.5 mm pellets for RE beam Mitigation (stage 3), all uniformly spaced at three different toroidal locations and multiple poloidal locations. The latter injectors, i.e. those dedicated to the mitigation of an existing RE beam (stage 3), cannot properly be studied in DREAM at this stage due to the lack
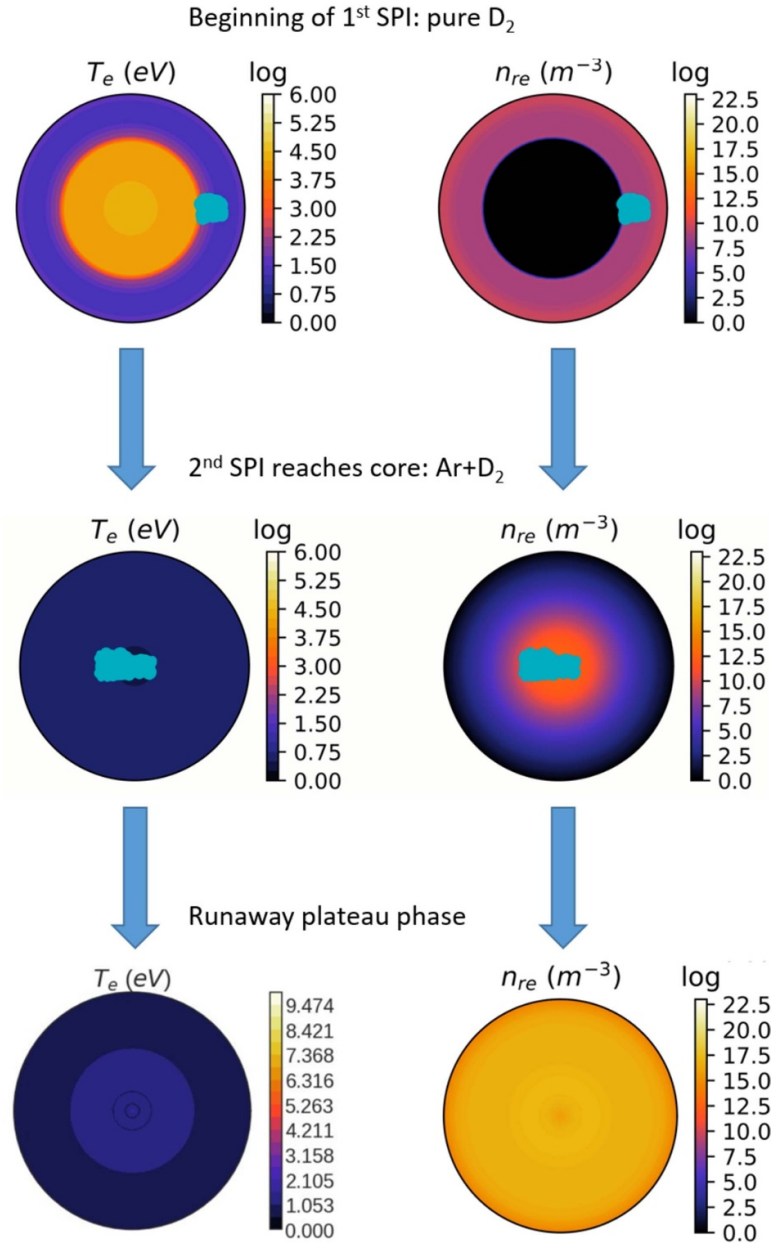
Figure 7. 2D representation of DREAM 1D modelling of a 2-stage SPI injection into STEP-EC-HD-v3, with $N_D = 2 \cdot 10^{23}$ atoms and $N_{Ar} = 4 \cdot 10^{21}$ atoms. The evolution of the cold electron temperature, T_e, is shown on the left and the evolution of the runaway electron density, n_{re}, on the right. Colourbar is in log10 (except for T_e in the RE plateau phase) and each pellet shard is represented by a cyan dot.

of MHD and molecular and atomic processes during the CQ phase (see [17]) so only the first two stages of injections are modelled in the following.

The number of shards used in the simulation is calculated during DREAM input file creation, using the Statistical Fragmentation Model [24].

Figure 7 shows such a simulation, with a subset of the 12×15 SPIs launched from the conformal wall, and the typical evolution of the electron temperature and the RE density. The first SPI injection of pure D_2 starts after 3 ms (with $v_{inj, \, D \, SPI} = 400 \, \text{m} \cdot \text{s}^{-1}$) and strongly dilutes the plasma, increasing the plasma density and decreasing the electron temperature to $\simeq 100 \, \text{eV}$. Compared to unmitigated disruptions

shown in section 2, the hot-tail generation of REs is reduced by orders of magnitude. However, both hot-tail and Dreicer generation are much higher than for the idealised impurity injections shown in the previous section. Then, the second SPI starts at 7 ms (with $v_{inj, \, Ar \, SPI} = 200 \, \text{m} \cdot \text{s}^{-1}$) and radiates almost all the plasma thermal energy. During that phase, we activate an ad-hoc 'MHD' TQ when the shards reach the $q = 3$ surface (by design, there is no q = 2 surface in STEP plasmas), lasting 1 ms (as in [18]) and with $\delta B/B = 2 \cdot 10^{-3}$ (as in section 3). Both the argon line radiation and the thermal transport due to 'MHD' decrease the electron temperature to a few eV post-TQ, as can be seen on figure 8. Unfortunately, a large RE beam carrying 12.7 MA of current is still generated.
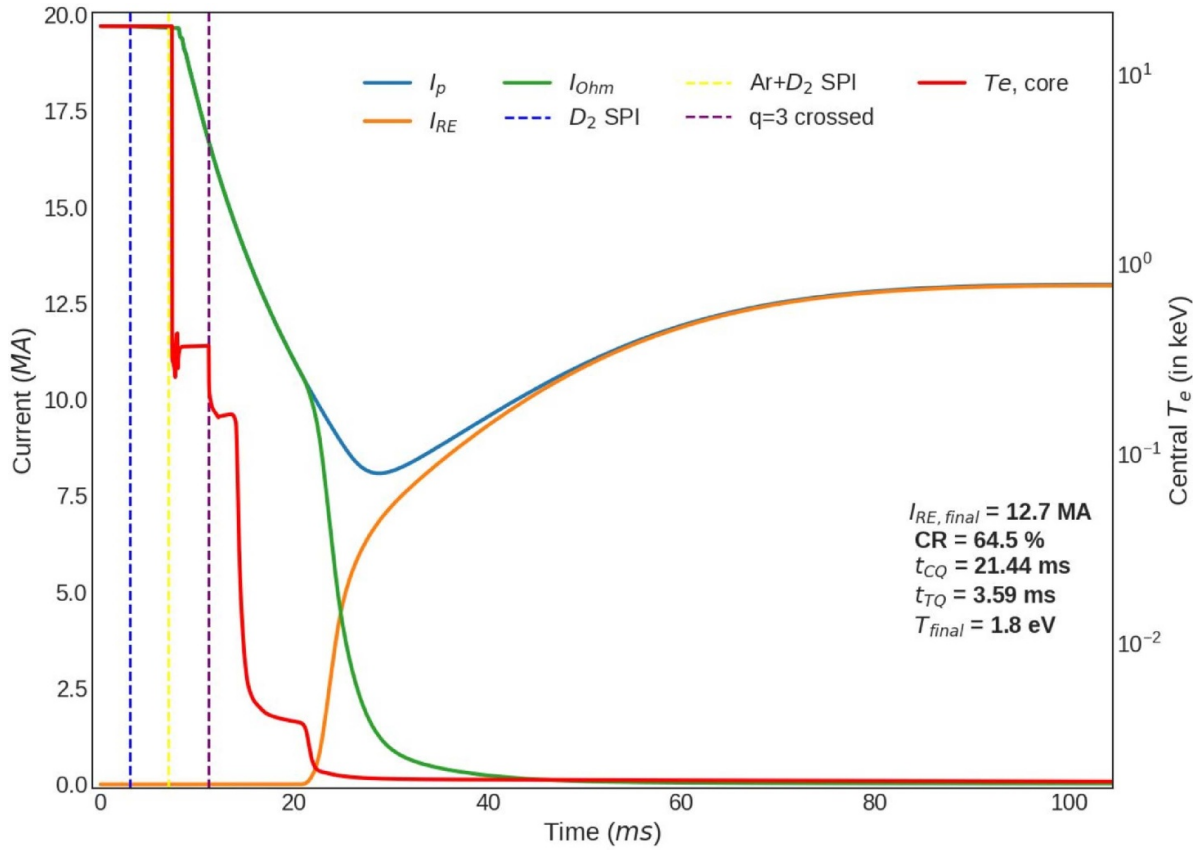
Figure 8. Two-stage SPI injection into STEP-EC-HD-v3, with $N_D = 2 \cdot 10^{23}$ atoms, $N_{Ar} = 4 \cdot 10^{21}$ atoms. Vertical dash lines indicate the start of the D_2 SPI (blue), the start of the argon SPI (yellow) and when the 2nd SPI shards cross the $q = 3$ surface (purple, after which a $\delta B/B = 2 \cdot 10^{-3}$ is applied during 1 ms). The evolution of the core electron temperature $T_{e,core}$, the total plasma current I_p, the ohmic current I_{Ohm} and the RE current I_{RE} is also shown.

Interestingly, the final RE current is quite insensitive to the number of injectors used (in the range of the initial STEP DMS concept). Studying the evolution of the pellet shards (see cyan dots in figure 7 as a example) shows that they are not fully assimilated (i.e. some shards fly through the plasma), even for the lowest injection quantities of the initial STEP DMS concept design (i.e. 1 injection of a pure 22 mm D_2 pellet, followed by 1 injection of a 16 mm argon pellet, when the maximum that can be injected is 12×15 injectors), motivating a reduction of the number (and/or size) of pellets injected. Simulations with a such reduced number show that we can reach full assimilation of the pellets, but a 12.5 MA RE beam is still obtained. When further reducing the injected argon quantities, we do not obtain a current quench anymore. Alternatively, reducing the first SPI D_2 quantities increases the final I_{RE} (through even higher hot-tail generation) up to 14.5 MA. These sets of simulations have been used to assess and improve STEP initial DMS concept design, but further optimisation is still possible through more extensive parameters scans (injections timings, injection velocities, etc). In particular, the higher hot-tail generation in the SPI cases compared to the idealised impurity injection suggest that further optimisation would require a more gradual assimilation of the D_2 shattered pellets in the plasma. Indeed, in the SPI cases, most of the hot-tail generation occurs between 4 and 8 ms,

i.e. before the ad-hoc TQ triggered by the $Ar + D_2$ SPI (usually at $t \simeq 11$ ms), and is due to the large and fast temperature drop caused by the D_2 SPI. An option would thus be to inject smaller successive pellets, to decrease the temperature more gradually. Such an extensive optimisation has been performed for ITER, in particular in [25] where a no-RE scenario was found (only without activated RE sources though). This should also be done for STEP, but the higher plasma current (20 vs 15 MA) will surely make the optimisation more challenging, and a no-RE scenario might still not exist (as suggested by the idealised impurity injections).

5. Discussion and conclusions

The results presented in section 4 and their modelling assumptions are further explored in this section. Adding Tritium in the simulations has only been tested on a few cases, but is found to increase the final RE current by up to 3 MA (i.e. 15.5 MA instead of 12.5 MA) for a 50/50 D-T mixture, through the additional RE source from tritium β decay. While not properly included so far as the total photon gamma flux has not yet been modelled in STEP, Compton scattering with the ITER photon gamma flux has been added to a few simulations and increases I_{RE} by less than 1 MA.
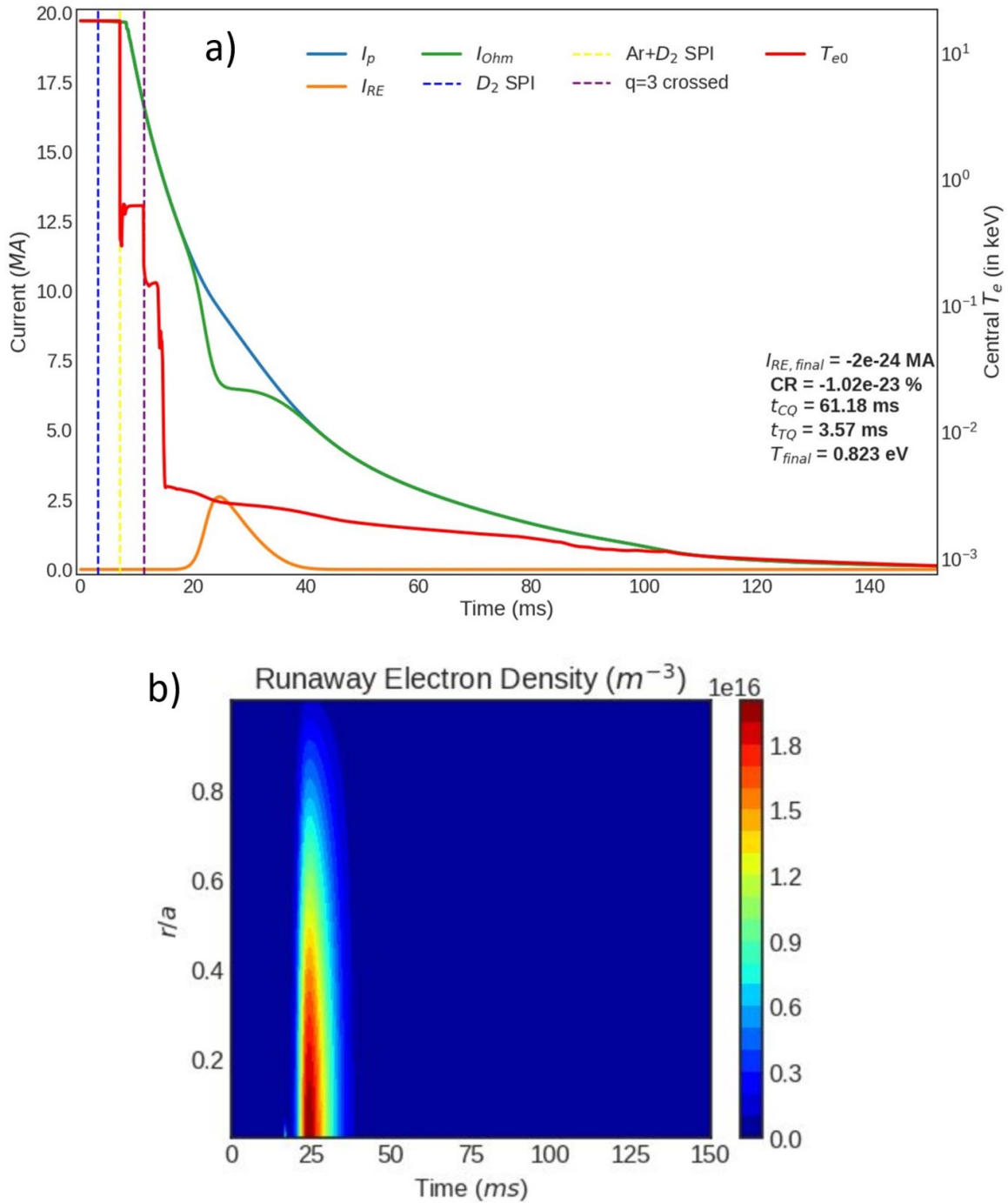
Figure 9. (*a*) Two-stage SPI injection into STEP-EC-HD-v3, with $N_D = 2 \cdot 10^{23}$ atoms, $N_{Ar} = 4 \cdot 10^{21}$ atoms and an ad-hoc REMC-like RE transport with $\delta B/B = 5 \cdot 10^{-4}$ during the full duration of the CQ. Vertical dash lines indicate the start of the D_2 SPI (blue), the start of the argon SPI (yellow) and when the 2nd SPI shards cross the q = 3 surface (purple, after which a $\delta B/B = 2 \cdot 10^{-3}$ is applied during 1 ms). The evolution of the core electron temperature $T_{e,core}$, the total plasma current I_p, the ohmic current I_{Ohm} and the RE current I_{RE} is also shown. (*b*) Evolution of the RE density profile, showing that a RE population is created after 20 ms before being depleted by the RE losses during the CQ.

Recent work has also shown that the hot-tail generation rate in DREAM fluid model could be overestimated for plasmas with low-Z (as the model was derived for high-Z) [26]. We have thus run a few STEP cases limiting the hot-tail generation (by two orders of magnitude), but this was found to only change the final RE current by a few % in our cases. Reducing it further (artificially) does however allow to reduce or even prevent the formation of the RE beam. To better model

the hot-tail generation, a few cases have also been run with DREAM isotropic model [10] (only for idealised impurity injections), which show a reduction of the final RE current, so we recommend future SPI cases to be done using DREAM kinetic models, to assess the validity of the fluid results.

Moreover, sensitivity scans of the TQ $\delta B/B$ (both amplitude and duration) have shown it can have a very large effect on the results. The cases presented in section 4 used a radially uniform $\delta B/B = 2 \cdot 10^{-3}$, applied for 1 ms, which resulted in a 12.7 MA RE beam. Compared to those, decreasing $\delta B/B$ increases I_{RE} progressively, up to 16.6 MA for $\delta B/B = 1 \cdot 10^{-4}$ (still applied for 1 ms). Increasing $\delta B/B$ higher than $2 \cdot 10^{-3}$, however, does not decrease I_{RE} substantially. Keeping $\delta B/B = 2 \cdot 10^{-3}$ but varying the 'MHD' TQ duration also changes the final I_{RE} (9 MA for 15 ms, 16 MA for 0.1 ms). This highlights the importance of performing high-fidelity 3D nonlinear MHD modelling of STEP mitigated disruptions in order to constrain and better justify the choice of RE transport parameters in DREAM (as was done for SPARC [4] or ITER [27], for example).

Finally, the simulations presented in this paper did not include the effect of plasmoid drifts. However, in STEP, the injectors of the first stage of the SPI scheme (pure D_2) are currently planned on the high field side of the device and we would thus expect a beneficial effect of plasmoid drifts on core assimilation of those pellets. A model to account for this, based on [28], has very recently been implemented in DREAM and the effect it has on the results presented in this paper will be studied next.

In conclusion, STEP DMS performance regarding RE generation and mitigation has been studied, and two-stage SPI injections are found to reduce hot-tail generation. However, these are currently not enough to avoid the formation of a large $\geqslant 10$ MA RE beam and further optimisation of the scheme is required. To mitigate potential RE beams, the STEP concept design already includes multiple D_2 SPI (with MGI as another option) systems dedicated to RE beam mitigation. This includes redundancy and assumes repetitive injections during the RE plateau to keep conditions prone to 'benign' termination of the RE beam [29] (i.e. keep the companion plasma recombined). While very preliminary, recent investigations using the 1D neutral diffusion model of [17] have shown that STEP mitigated disruptions could be in such a regime, with the need of only a limited amount of CQ injections. While the potential of such a scheme has been demonstrated on existing fusion devices such as JET [30], further extensive modelling of STEP using 3D non-linear MHD codes such as JOREK [31] is essential and very high priority for the STEP programme.

Experimental results from ITER and SPARC will also be essential to validate and optimise STEP DMS. In particular, passive and/or active 3D fields induced during the CQ could reduce substantially RE generation, and STEP is looking at the possibility of integrating a RE mitigation coil (REMC). Such coils have been modelled and designed for DIII-D and SPARC [4, 6, 32], showing promising results. Initial STEP simulations based on the one in figure 8 show that a value of $\delta B/B = 5 \cdot 10^{-4}$ during the CQ is enough to prevent the formation of the RE beam (see figure 9). However, islands

reformation [33], actual duration of the CQ stochastic phase, and proper modelling of REMC fields have only just started and are now high-priority for the STEP programme.

ORCID iDs

A. Fil ⬤ https://orcid.org/0000-0001-5755-4440
M. Hoppe ⬤ https://orcid.org/0000-0003-3994-8977
O. Vallhagen ⬤ https://orcid.org/0000-0002-5444-5860

References

[1] Lehnen M. *et al* 2015 Disruptions in ITER and strategies for their control and mitigation *J. Nucl. Mater.* **463** 39–48
[2] Meyer H. 2024 Plasma burn—mind the gap *Phil. Trans. R. Soc. A.* **382** 20230406
[3] Vallhagen O., Pusztai I., Hoppe M., Newton S.L. and Fülöp T. 2022 Effect of two-stage shattered pellet injection on tokamak disruptions *Nucl. Fusion* **62** 112004
[4] Tinguely R.A. *et al* 2021 Modeling the complete prevention of disruption-generated runaway electron beam formation with a passive 3D coil in SPARC *Nucl. Fusion* **61** 124003
[5] Berger E., Pusztai I., Newton S.L., Hoppe M., Vallhagen O., Fil A. and Fülöp T. 2022 Runaway dynamics in reactor-scale spherical tokamak disruptions *J. Plasma Phys.* **88** 905880611
[6] Izzo V.A., Pusztai I., Särkimäki K., Sundström A., Garnier D.T., Weisberg D., Tinguely R.A., Paz-Soldan C., Granetz R.S. and Sweeney R. 2022 Runaway electron deconfinement in SPARC and DIII-D by a passive 3D coil *Nucl. Fusion* **62** 096029
[7] Liu Y., Aleynikova K., Paz-Soldan C., Aleynikov P., Lukash V. and Khayrutdinov R. 2022 Toroidal modeling of runaway electron loss due to 3-D fields in ITER *Nucl. Fusion* **62** 066026
[8] Bandaru V., Hoelzl M., Reux C., Ficker O., Silburn S., Lehnen M. and Eidietis N. 2021 Magnetohydrodynamic simulations of runaway electron beam termination in JET *Plasma Phys. Control. Fusion* **63** 035024
[9] Liu C., Zhao C., Jardin S.C., Ferraro N.M., Paz-Soldan C., Liu Y. and Lyons B.C. 2021 Self-consistent simulation of resistive kink instabilities with runaway electrons *Plasma Phys. Control. Fusion* **63** 125031
[10] Hoppe M., Embreus O. and Fülöp T. 2021 DREAM: a fluid-kinetic framework for tokamak disruption runaway electron simulations *Comput. Phys. Commun.* **268** 108098
[11] Cunningham G. 2013 High performance plasma vertical position control system for upgraded MAST *Fusion Eng. Des.* **88** 3238–47
[12] Miller R.L., Chu M.S., Greene J.M., Lin-Liu Y.R. and Waltz R.E. 1998 Noncircular, finite aspect ratio, local equilibrium model *Phys. Plasmas* **5** 973–8

[13] Fülöp T., Helander P., Vallhagen O., Embreus O., Hesslow L., Svensson P., Creely A.J., Howard N.T. and Rodriguez-Fernandez P. 2020 Effect of plasma elongation on current dynamics during tokamak disruptions *J. Plasma Phys.* **86** 474860101

[14] Hesslow L., Unnerfelt L., Vallhagen O., Embreus O., Hoppe M., Papp G. and Fülöp T. 2019 Evaluation of the Dreicer runaway generation rate in the presence of high-impurities using a neural network *J. Plasma Phys.* **85** 475850601

[15] Hesslow L., Embréus O., Vallhagen O. and Fülöp T. 2019 Influence of massive material injection on avalanche runaway generation during tokamak disruptions *Nucl. Fusion* **59** 084004

[16] Rechester A.B. and Rosenbluth M.N. 1978 Electron heat transport in a tokamak with destroyed magnetic surfaces *Phys. Rev. Lett.* **40** 38–41

[17] Hollmann E.M. *et al* 2023 Trends in runaway electron plateau partial recombination by massive H_2 or D_2 injection in DIII-D and JET and first extrapolations to ITER and SPARC *Nucl. Fusion* **63** 036011

[18] Hu D., Nardon E., Hoelzl M., Wieschollek F., Lehnen M., Huijsmans G.T.A., van Vugt D.C. and Kim S.-H. 2021 Radiation asymmetry and MHD destabilization during the thermal quench after impurity shattered pellet injection *Nucl. Fusion* **61** 026015

[19] Hesslow L., Embréus O., Wilkie G.J., Papp G. and Fülöp T. 2018 Effect of partially ionized impurities and radiation on the effective critical electric field for runaway generation *Plasma Phys. Control. Fusion* **60** 074010

[20] Lehnen M. *et al* 2021 DMS heat load mitigation targets *ITER Report* 57VT5Y

[21] Sheikh U. *et al* 2024 Benign termination of runaway electron beams on ASDEX Upgrade and TCV *Plasma Phys. Control. Fusion* **66** 035003

[22] Sugihara M., Shimada M., Fujieda H., Gribov Y., Ioki K., Kawano Y., Khayrutdinov R., Lukash V. and Ohmori J. 2007 Disruption scenarios, their mitigation and operation window in ITER *Nucl. Fusion* **47** 337–52

[23] Matsuyama A., Sakamoto R., Yasuhara R., Funaba H., Uehara H., Yamada I., Kawate T. and Goto M. 2022 Enhanced material assimilation in a toroidal plasma using mixed H_2 + Ne pellet injection and implications to ITER *Phys. Rev. Lett.* **129** 255001

[24] Gebhart T.E., Baylor L.R. and Meitner S.J. 2020 Shatter thresholds and fragment size distributions of deuterium–neon mixture cryogenic pellets for tokamak thermal mitigation *Fusion Sci. Technol.* **76** 831–5

[25] Vallhagen O., Hanebring L., Artola J., Lehnen M., Nardon E., Fülöp T., Hoppe M., Newton S. and Pusztai I. 2024 Runaway electron dynamics in ITER disruptions with shattered pellet injections (arXiv:2401.14167)

[26] Ekmark I., Hoppe M., Fülöp T., Jansson P., Antonsson L., Vallhagen O. and Pusztai I. 2024 Fluid and kinetic studies of tokamak disruptions using Bayesian optimization *J. Plasma Phys.* **90** 905900306

[27] Hu D., Nardon E., Artola J., Lehnen M., Bonfiglio D., Hoelzl M., Huijsmans G. and Lee S.J. 2023 Collisional-radiative simulation of impurity assimilation, radiative collapse and MHD dynamics after ITER shattered pellet injection *Nucl. Fusion* **63** 066008

[28] Vallhagen O., Pusztai I., Helander P., Newton S.L. and Fülöp T. 2023 Drift of ablated material after pellet injection in a tokamak *J. Plasma Phys.* **89** 905890306

[29] Paz-Soldan C. *et al* 2021 A novel path to runaway electron mitigation via deuterium injection and current-driven MHD instability *Nucl. Fusion* **61** 116058

[30] Reux C. *et al* 2022 Physics of runaway electrons with shattered pellet injection at JET *Plasma Phys. Control. Fusion* **64** 034002

[31] Hoelzl M. *et al* 2021 The JOREK non-linear extended MHD code and applications to large-scale instabilities and their control in magnetically confined fusion plasmas *Nucl. Fusion* **61** 065001

[32] Battey A., Hansen C., Garnier D., Weisberg D., Paz-Soldan C., Sweeney R., Tinguely R. and Creely A. 2024 Design of passive and structural conductors for tokamaks using thin-wall eddy current modeling *Nucl. Fusion* **64** 016010

[33] Tinguely R.A. *et al* 2023 On the minimum transport required to passively suppress runaway electrons in SPARC disruptions *Plasma Phys. Control. Fusion* **65** 034002